Available online at www.sciencedirect.com

ScienceDirect

Energy Procedia 48 (2014) 689 – 700

Energy Procedia

SHC 2013, International Conference on Solar Heating and Cooling for Buildings and Industry
September 23-25, 2013, Freiburg, Germany

Seasonal performance of a combined solar, heat pump and latent heat storage system

Christian Winteler[a,]*, Ralf Dott[a], Thomas Afjei[a], Bernd Hafner[b]

[a]*Institut Energie am Bau, Fachhochschule Nordwestschweiz FHNW, St. Jakobs-Strasse 84, CH-4132 Muttenz, Switzerland*
[b]*Viessmann Werke GmbH & Co KG, D-35107 Allendorf, Germany*

Abstract

This paper investigates the seasonal performance of a combined solar, heat pump and ice storage system for residential dwellings. A simulation study is performed for seven different heat loads, i.e. building types, ranging from low-energy buildings to non-renovated existing buildings. Four reference buildings suitable for this heat generation system are presented and discussed in this paper. In addition, the solar ice system is applied to the three reference buildings defined in IEA HPP Annex 38 / SHC Task 44 "Solar and heat pump systems". The simulation results show that the solar ice storage system generates heat efficiently for a large variety of heat loads and consistently reaches a seasonal performance factor comparable to heat pump systems with borehole heat exchangers, i.e. SPF ~ 4.

Selection and peer review by the scientific conference committee of SHC 2013 under responsibility of PSE AG

Keywords:solar heat; heat pump; latent heat; ice storage

1. Introduction

The turnaround in energy policy demands energy supply systems to use predominantly renewable energy sources. Heat pumps in combination with solar energy are key technologies for heat generation for space heating and domestic hot water in buildings. Currently the most effective heat sources for heat pumps are borehole heat

* Corresponding author. Tel.: +41 61 467 47 09; fax: +41 61 467 45 43.
E-mail address: christian.winteler@fhnw.ch

1876-6102
Selection and peer review by the scientific conference committee of SHC 2013 under responsibility of PSE AG
doi:10.1016/j.egypro.2014.02.080

exchangers. Recently systems with large ice storages have been promoted as equally efficient at comparable cost without the need for deep drilling and the associated authorization and risks. Furthermore, ice storages can also be installed in areas where deep drilling is not possible or prohibited, even in water protection areas since the ice storage is filled with pure water.

Aim of this study is to investigate the seasonal performance of a combined solar, heat pump and ice storage system for buildings with different heat loads and to compare it to the average seasonal performance factor of systems with borehole heat exchangers of ~ 4.0.

Nomenclature

DHW	domestic hot water
SFH	single family house
SPF	seasonal performance factor

2. Methods

The work presented here is conducted as simulation study validated with laboratory and field measurements. Figure 1 shows a schematic representation of the solar ice heat generation system. The central component is a brine/water heat pump that supplies heat for space heating, as well as for DHW preparation. The primary source of the heat pump is an uncovered thermal absorber that generates heat from solar irradiation as well as from convective gains. A buried ice storage serves as alternative heat source for the heat pump in case the absorber cannot supply the necessary heat. In the ice storage heat is predominantly stored as latent heat, i.e. in the phase transition from water to

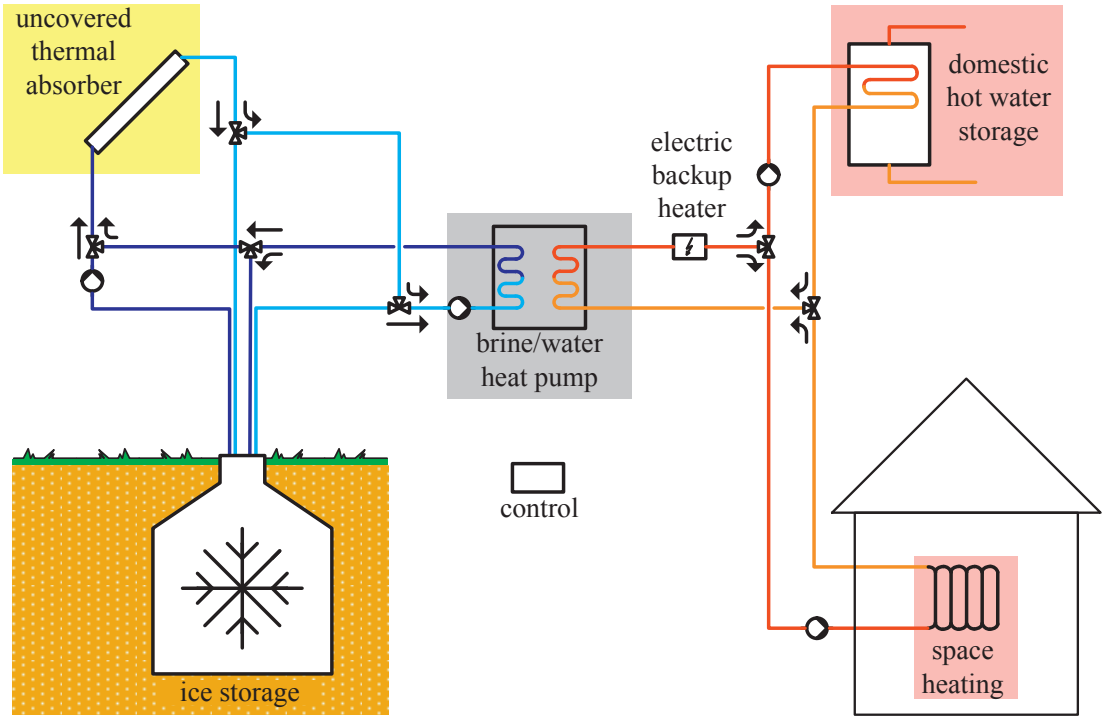

Figure 1: System and hydraulic scheme

ice. Excess heat from the absorber is used to recharge the ice storage. Additionally, the ice storage also gains heat from the surrounding soil. In the case of source temperatures below the operational limit of the heat pump an electric backup heater guarantees heat supply.

The simulation models of this system have been validated with laboratory and field test data. Heat generated by the heat pump is used for space heating and domestic hot water preparation of a single family house. Heat pump models intended by the manufacturer for the solar ice storage system have thermal capacities of 6, 8, 10 and 13 kW. Therefore four reference buildings with corresponding heat loads (including domestic hot water preparation) were defined and are discussed in detail in Section 3. These buildings are labeled SFH25*, SFH45*, SFH60* and SFH100* where the numbers refer to the space heat demand in kWh/m^2/a. These building types will be referred to as *SolEis-buildings*. The superscript asterisk is used to discern the aforementioned building types and the reference buildings defined in IEA HPP Annex 38 / SHC Task 44 "Solar and heat pump systems" [3,4] called SFH15, SFH45 and SFH100, which are also employed in this study and will be referred to as *Task-buildings*. The implementation of the *Task-buildings* in the presented simulation environment slightly differs from the reference which can lead to an increase in the heat demand due to a different space heating control. However, the aim of the study is not to perfectly match the heat load to the reference [1], but to investigate the behavior of the heat generation system for different system configurations.

2.1. Applied tools and parameter data sets

All simulations are performed with MATLAB®/SIMULINK® [1] in combination with the CARNOT Blockset [2], an extension for the calculation and simulation of thermal components of heating systems. All simulation results are annual values from July to July with 300 days preconditioning, corresponding to one full heating period. Heat loads are simulated with the simple house model from the CARNOT Blockset parameterized according to the building definitions from the previous chapter or from IEA HPP Annex 38 / SHC Task 44. The Isocal solar ice system [5] consists of Isocal SLK-S pipe absorber modules and an Isocal SES ice storage.

The absorber is modeled as described in [6] and parameterized according to the data in [5]. Effects of condensation as well as freezing/frosting are not taken into account. The model has been validated through laboratory tests both with and without irradiation. For the brine/water heat pump the generic heat pump model from the CARNOT Blockset is used with performance data of Viessmann Vitocal 300 G BW series models [7] BW 301.A06 (6 kW), BW 301.A08 (8 kW), BW 301.A10 (10 kW) and BW 301.A13 (13 kW). The storage tank model is a CARNOT multiport model with specifications of a Viessmann Vitocell 100-V CVW [8]. All simulation models and applied parameter data sets have furthermore been validated through field test measurement data.

3. SolEis-building model specifications

In order to investigate the performance of the solar ice storage system under near ideal conditions the heat load both for space heating and DHW preparation and the thermal capacity of the heat pump should match. Since there are four heat pump types intended by the manufacturer for the solar ice system, four building types were defined specifically for this study. The building models are derived from the reference models presented in [3]. All building types employed in this study share the same general building geometry which is shown in Figure 2. In contrast to the Task-buildings, the SolEis-buildings have a net floor area (first plus second floor) of 250 m^2, which leads to different overall building measures. All SolEis-buildings share the same geometrical structure fixed by inside measures. This common, independent geometry is summarized in Table 1. The different building types are then derived by applying different insulation thicknesses resulting in specific measures as summarized in Table 2. A detailed view of the building structure and naming convention is shown in Figure 3. Internal walls and floors are only depicted for the sake of completeness and are only considered as thermal mass in the simulation. All buildings are simulated as one homogeneous thermal zone. The thermal capacity of the buildings is set to 0.5 MJ/m^2. Simulations are based on inside measures, no additional thermal bridges are considered. Building envelope areas are summarized in Table 3.

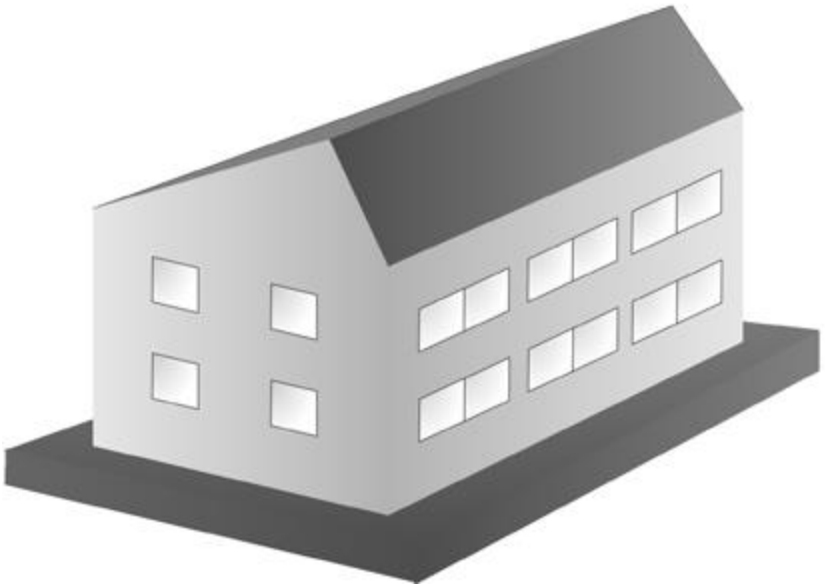

Figure 2: Simple view of the house (showing South and West facades) [3].

Table 1:Building type independent geometry according to Figure 3.

part	a	b	f	g	h	m	n	r	α	β
measure	7.81 m	3.78 m	10 m	12.5 m	2.6 m	0.4 m	0.2 m	2.67 m	45°	20°

Table 2: Building type specific geometry according to Figure 3.

part	building	c	d	e	j	k	s
measure	SFH25*	10.86 m	13.36 m	6.11 m	0.43 m	0.51 m	0.26 m
	SFH45*	10.66 m	13.16 m	6.01 m	0.33 m	0.41 m	0.16 m
	SFH60*	10.62 m	13.12 m	5.95 m	0.31 m	0.35 m	0.12 m
	SFH100*	10.54 m	13.04 m	5.97 m	0.27 m	0.37 m	0.08 m

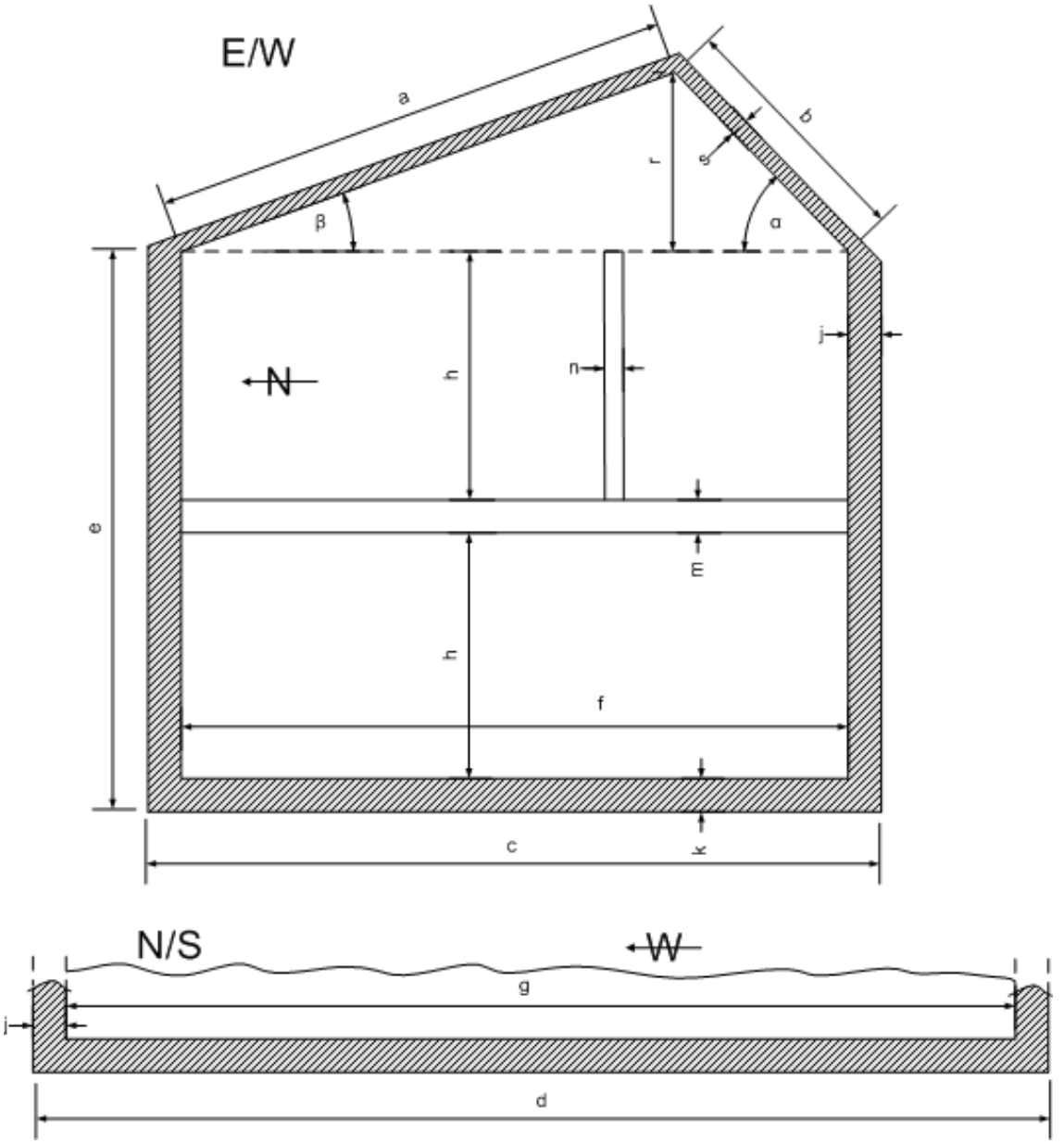

Figure 3: View of the E/W section of the building with naming convention (top), cropped view of the N/S section (bottom). The hatched components play an active part in the simulation in terms of heat losses and geometry, the other parts are only considered as thermal mass without their individual geometry [1].

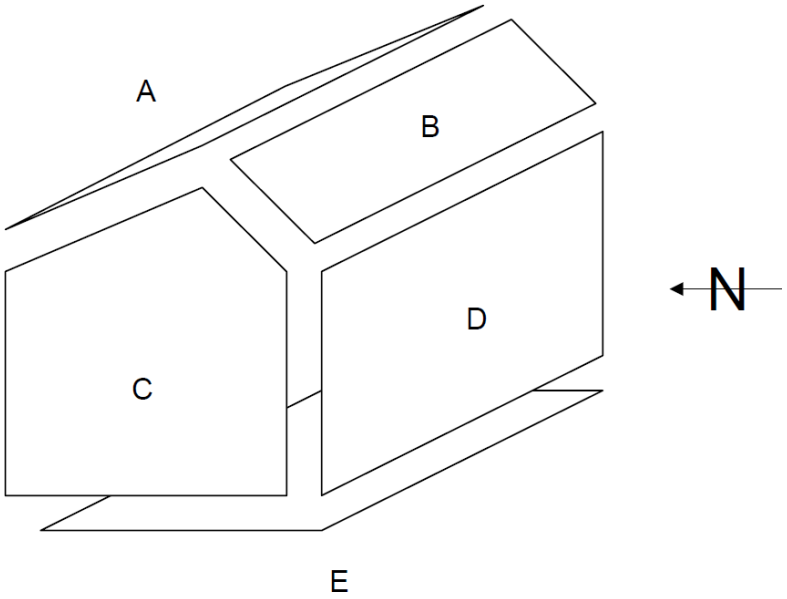

Figure 4: View of the envelope parts with naming convention for the areas.

Table 3: Inside and outside areas of the building envelope according to Figure 4

	building	A =d*a	B =d*b	C =c*(e+r/2)	D =d*e	E =d*c
net (inside) area (m^2)	all	97.6	47.2	69.4	70.0	125.0
gross (outside) area (m^2)	SFH25*	104.3	50.4	80.8	81.5	145.0
	SFH45*	102.7	49.7	78.2	79.0	140.2
	SFH60*	102.4	49.5	77.3	78.0	139.2
	SFH100*	101.8	49.2	76.9	77.8	137.3

3.1. Construction of building elements

3.1.1. Opaque elements

The construction of opaque building elements (walls, floors, and roof) is described in Table 4. U-value calculations are based on EN ISO 6946, using a total heat transfer coefficient $\alpha_i = 7.69$ W/m^{2}K to the inside and $\alpha_e = 25.0$ W/m^{2}K to the outside.

Table 4: Construction of opaque building elements.

assembly	layer	layer thickness (m)				density (kg/m^3)	conductivity (W/mK)	capacity (kJ/KgK)	U-value construction (W/m^{2}K)			
		SFH25*	SFH45*	SFH60*	SFH100*				SFH25*	SFH45*	SFH60*	SFH100*
external wall	Plaster inside		0.015			1200	0.600	1.00	0.18	0.33	0.40	0.67
	Brick		0.210			1380	0.700	1.00				
	EPS	0.200	0.100	0.080	0.040	17	0.040	0.70				
	Plaster outside		0.003			1800	0.700	1.00				
ground floor	wood		0.015			600	0.150	2.50	0.14	0.21	0.33	0.33
	plaster floor		0.080			2000	1.400	1.00				
	sound insulation		0.040			80	0.040	1.50				
	concrete		0.150			2000	1.330	1.08				
	XPS	0.220	0.120	0.060	0.060	38	0.037	1.45				
roof ceiling	gypsum board		0.025			900	0.211	1.00	0.16	0.28	0.41	0.77
	plywood		0.015			300	0.081	2.50				
	rock wool	0.200	0.100	0.060	0.020	60	0.036	1.03				
	plywood		0.150			300	0.081	0.92				

3.2. Reference conditions

The reference conditions of [3,4] are applied for all building types using the following options and modifications:

- Domestic hot water preparation is delivered by a boiler with attached mixing valve to adjust the fixed tapping temperature and heated only by the heat pump. Storage temperature is set to 50 °C. For small storages (≤ 400 l) water circulation and renewal is assumed to be sufficient to prevent pathogen growth (Legionella).
- The seasonal variation of the DHW energy demand is approximated by a sine-curve variation of the cold water temperature around a mean value of 10 °C with amplitude 3 °C and phase shift -137 days.
- The heating characteristic of the heat pump controller defines the space heating return flow temperature as a function of the outdoor temperature. The heating characteristic is set such that the room temperature is kept around 20 ± 0.5 °C. If necessary, DHW preparation has priority over space heating.
- Solar thermal absorber modules are installed on a south facing roof at an inclination of 40°.

For SolEis-buildings, the following options or modifications are used:

- Moderate climate of Wuerzburg, a German city in central Europe.
- Simplified DHW tapping profile of only three tappings per day (07:00, 12:00 and 19:00) corresponding to an average draw-off of 200 l/d at 45 °C or 7.964 kWh/d (2907 kWh/a).
- The heat delivery system for space heating in SFH25*, SFH45* and SFH60* is a floor heating system, in SFH100* a radiator. The required flow temperatures needed to satisfy the heat demands at design outdoor temperature are 30 °C for the SFH15* building, 33 °C for the SFH45*, 41°C for the SFH60* building and 48 °C for the SFH100* building (cf. Table 5).

- Internal heat gains are approximated by a constant heat gain of 2.557 W/m^2.
- Heat losses through the ground floor are calculated using a constant earth temperature of 10 °C.
- The collector area for the buildings SFH25*, SFH45* and SFH60* amounts to approximately 10 m^2, for building SFH100* to 20 m^2.

The following options and modifications are used for the Task-buildings:

- Moderate climate of Strasbourg, a French city in central Europe
- Simplified DHW tapping profile of only three tappings per day (07:00, 12:00 and 19:00) corresponding to an average draw-off of 140 l/d at 45 °C or 5.845 kWh/d (2133 kWh/a).
- The heat delivery system for space heating in SFH15 and SFH45 is a floor heating system, in SFH100 a radiator. The required flow temperatures needed to satisfy the heat demands at design outdoor temperature are 30 °C for the SFH15 building, 34 °C for the SFH45 and 48 °C for the SFH100 building (cf. Table 5).
- There is a range of heat pump models intended by the manufacturer for the solar ice storage system with thermal capacities of 6, 8, 10 and 13 kW. To study the behaviour of the heat generation system in combination with the aforementioned reference buildings, a heat pump is chosen for each building such that its thermal capacity exceeds the design heat load of the building (1.8 kW, 4 kW and 7.3 kW for SFH15, SFH45 and SFH100 respectively).
- The collector area for the buildings SFH15 and SFH45 amounts to approximately 10 m^2, for building SFH100 to 20 m^2.

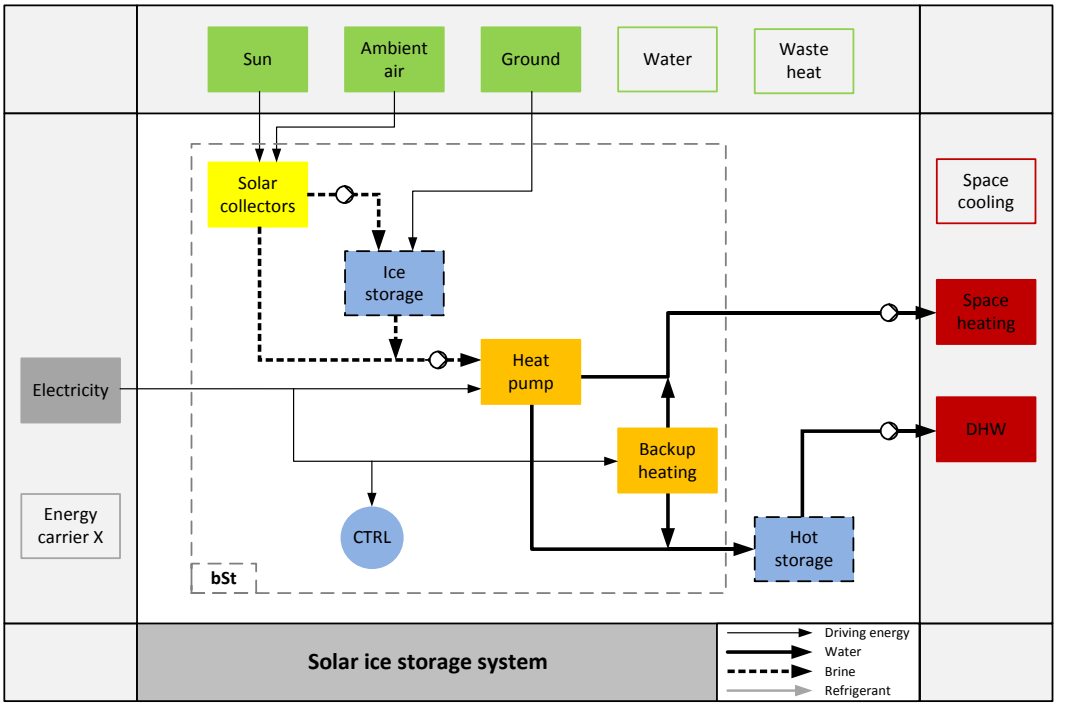

Figure 5: Visualization of the energy flows of the solar ice storage heating system. The dashed square indicates the system boundary for the calculation of the SPF. The representation method is based on [10].

4. Simulation results

The System boundary for the performance factor calculation includes all components of the system excluding the heating and DHW distribution systems. Figure 5 shows a visualization of the energy flows and the system boundary. The system boundary corresponds to *system boundary bSt - before storage* according to the definitions in [5]. It is a measure for the performance of the system without the influence of storage losses and the energy distribution system, which is generally different for every installation site and cannot be influenced by the manufacturer or installer of a SHP system [5].

The corresponding seasonal performance factor is labeled $\mathbf{SPF_{bSt}}$ and is defined as:

$$SPF_{bSt} = \frac{\int\left(\dot{Q}_{HP,SH} + \dot{Q}_{HP,DHW} + \dot{Q}_{BU,SH} + \dot{Q}_{BU,DHW}\right)\cdot dt}{\int\left(\sum P_{el,SHP}\right)\cdot dt}, \text{ with} \qquad (1)$$

$$\sum P_{el,bSt} = P_{el,sol} + P_{el,HPSrc} + P_{el,HP} + P_{el,BU} + P_{el,CTRL}$$

A selection of results for the three chosen systems is presented in Figure 6 and Table 5. Therein, the following results are shown:

- The total generated heat for space heating and domestic hot water preparation in kilowatt-hours (kWh), divided into the different heat sources for the heat pump: electricity, solar collector or ice storage. The contribution from the ice storage is subdivided into a solar and a ground heat part, depending on how the heat extracted from the ice storage is restored. Since heat exchange between ice storage and ground works in both ways, the displayed value denotes the net annual energy balance. The latent heat contribution cannot be displayed here since its annual energy balance is zero.
- The seasonal performance factor SPF_{bSt} of the heat generation system according to Eq.(1).

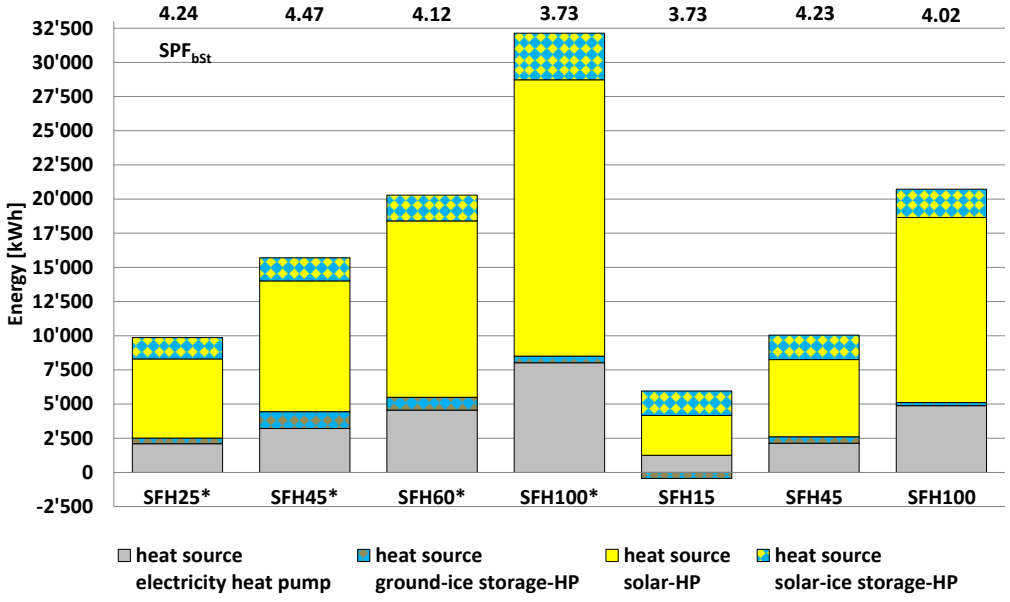

Figure 6: Annual energy balance of the heat generation system (heat pump, solar collector and ice storage).Usable energy is depicted on the ordinate axis, subdivided into the different heat sources of the heat pump. Negative values indicate a net heat loss from the ice storage to the ground.

For most building types, a system configuration could be found that yields a $SPF_{bSt} > 4$. Only for the building types with the highest (SFH100*) and the lowest (SFH15) heat demand the desired SPF_{bSt} could not be reached. Various factors that have a negative effect on the efficiency in these systems will be presented in the next section.

The breakdown of heat pump heat sources in Figure 6 shows that the predominant source in all systems is the solar collector. Heat extracted from the ice storage is also chiefly regenerated by the collectors; the net ground heat contribution is usually significantly lower.

Component dimensions are listed in Table 5. Due to the very high heat demand of the SFH100* variant, a second ice storage had to be installed to ensure heat generation without the need for direct electric backup heating throughout the year.

Table 5: System simulation results.

Building type	Design heat load in kW	Ice storage volume in m^3	Solar absorber area in m^2	Thermal power of heat pump in kW	Total generated heat in kWh	Design flow/return temperature in °C	Total generator electricity consumption in kWh	SPF of heat generator
SFH25*	5.5	10	10	6	9'558	30/25	2'254	4.24
SFH45*	7.5	10	13	8	15'257	33/28	3'413	4.47
SFH60*	9.5	10	20	10	19'784	41/31	4'800	4.12
SFH100*	12.5	20	30	13	31'439	48/38	8'428	3.73
SFH15	1.8	10	10	6	5'250	30/25	1'412	3.73
SFH45	4.0	10	10	6	9'731	34/29	2'301	4.23
SFH100	7.3	10	20	10	20'249	48/38	5'040	4.02

5. Discussion

The simulation study yields good seasonal performance factors for all system configurations. Since the direct electric backup heater is very inefficient in generating heat, it should be used as little as possible or better not at all. In all presented simulations, the ice storage did not freeze completely which in turn means that the source temperature did not drop below the operational limit of the heat pump and hence no direct electric heating was necessary.

The building types SFH25*, SFH15 and SFH45 were all simulated using the same heat generator configuration (Heat pump capacity, absorber area and ice storage volume), but resulted in a different SPF_{bSt}. For SFH25* and SFH45 about the same amount of heat was generated which resulted in an almost identical SPF_{bSt}, even though the design flow and return temperatures of SFH45 were slightly higher. However, the SPF_{bSt} for SFH15 is significantly lower, even below the targeted 4. Due to the high insulation quality of this building type, very little heat is needed for space heating and in turn the share of heat generated for DHW preparation is around 40 %. Since significantly higher temperatures are needed for DHW preparation, this has a lowering effect on the SPF. In addition, the electricity consumption of auxiliary systems (control, solar pump and heat pump source pump) is about equal for all three building types, but due to the low heat production for SFH15, there the negative effect on the SPF is much larger.

For the building types with radiator heating systems (SFH100* and SFH100) flow and return temperatures are higher than for floor heating systems. This in turn leads to a reduction of the SPF. In addition, the higher the thermal power of the heat pump, the higher source mass flow rates are needed. To provide these mass flow rates more powerful pumps are needed which also consume more electric energy and therefore the SPF is reduced.

A detailed graphical unraveling of the heat pump heat sources is shown in Figure 6. The solar absorbers are the primary heat source for the heat pump in all simulations. Since the absorber area is in general increasing with increasing heat pump capacity also the heat contribution from the absorbers is increasing. In contrast, the fraction of heat extracted from the ice storage that is regenerated with solar is roughly proportional to the size of the ice storage.

The contribution from the ground is significantly lower than the solar contribution to the ice storage and it varies much more among the different simulations. Since heat exchange with the ground works in both directions, the annual energy balance only shows half the picture. Figure 7 shows the monthly energy balance of the ice storage in the SFH45* simulation. From May to October the ice storage is warmer than the surrounding ground and loses heat to the ground. At the same time the highest solar gains occur, but are almost completely lost to the ground except for some heating of the water occurring in May. At the beginning of the heating period (October until March), the ice storage is quickly cooled below ground temperature (in October and November) resulting in heat gains from the ground during the rest of the period. While latent heat is extracted from November to January, thawing already starts in February and ends somewhere around April. Outside the heating period, only little heat is extracted from the ice storage by the heat pump.

6. Conclusion

Specific building models for the ice storage heating system were designed and simulated together with the reference building models from [3]. The simulation study shows, that the solar ice system generates heat efficiently for different heat loads and under different climatic conditions. It reaches $SPF_{bSt} > 4$ for buildings with moderate (SFH25*) to high (SFH100*) space heat demands with space heating or radiator heat delivery systems. The system is not primarily intended for buildings with very low heat loads (SFH15) but reaches a SPF_{bSt} close to 4 nevertheless.

Solar heat is the primary heat source for the heat pump. The ice storage stores solar heat and serves as source for the heat pump during the heating period. Heat exchange with the ground plays an important role in preventing complete freezing of the ice storage in winter hence there is no need for inefficient direct electric heating. We expect to be able to compare the simulation results to real world installations in the near future.

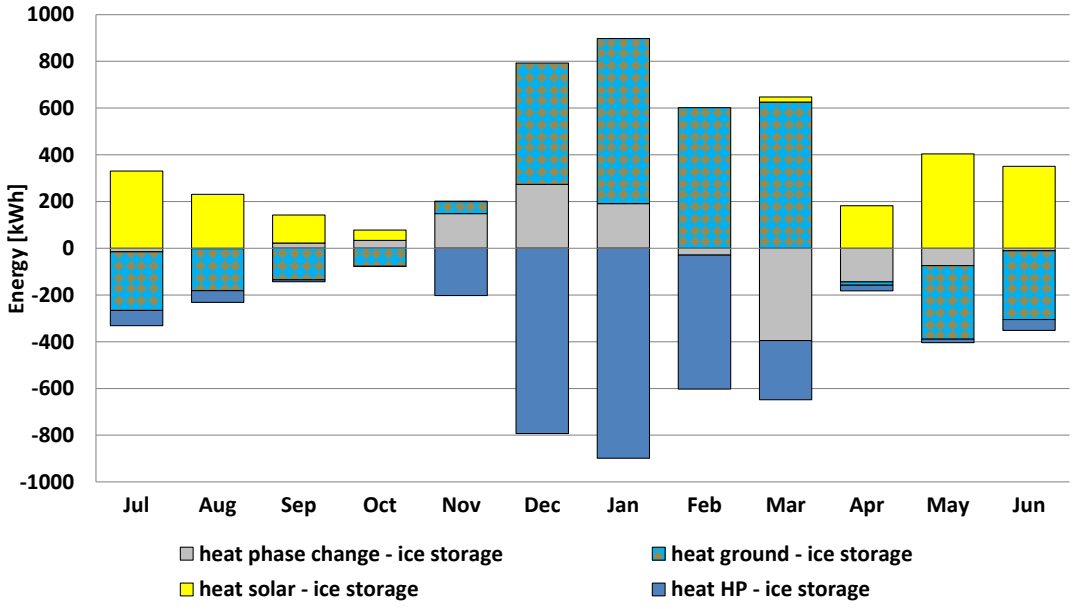

Figure 7: Monthly energy balance of the ice storage of simulation SFH45*. Heat exchange is depicted on the ordinate axis, subdivided into the different exchange partners. Positive values indicate heat flow to the ice storage. Phase change gains (losses) describe energy released (lost) through cooling (heating) or freezing (thawing) of water/ice.

Acknowledgements

The authors are grateful for the project advising and funding by the Swiss Federal Office of Energy SFOE in the frame of the project SOFOWA. They acknowledge the support of the component manufacturers Viessmann Werke GmbH & Co. KG and isocal HeizKühlsysteme GmbH. The project contributes to the IEA SHC Task 44 / HPP Annex 38 “Solar and heat pumps”. The permission of Meteotest for using Meteonorm climate data for simulations within the IEA SHC Task 44 / HPP Annex 38 is gratefully acknowledged

References

[1] Matlab®/Simulink® Version R2011b, The Mathworks, Inc.
[2] CARNOT Toolbox für Matlab/Simulink Ver. 5.2, August 2012.
[3] Dott R, Haller MY, Ruschenburg J, Ochs F, Bony J. Reference Buildings Description of the IEA SHC Task 44 / HPP Annex 38. ; 2011.
[4] Haller MY, Dott R, Ruschenburg J, Ochs F, Bony J. The Reference Framework for System Simulations of the IEA SHC Task 44 / HPP Annex 38. ; 2011.
[5] Das Wärmequellensystem SE 12 - Informationsblatt, isocal HeizKühlsysteme GmbH, Friedrichshafen, Deutschland, 2012.
[6] Frank E. Modellierung und Auslegungsoptimierung unabgedeckter Solarkollektoren für die Vorerwärmung offener Fernwärmenetze: Kassel University Press; 2007.
[7] Data set for Viessmann Vitocal 300-G BW series , in Planungsunterlagen für Wärmepumpen - Ausgabe 05/2012, Viessmann Deutschland GmbH, Allendorf, Germany, 2012.
[8] Datenblatt Viessmann Vitocell 100-V Typ CVW - 06/2009, Viessmann Deutschland GmbH, Allendorf, Germany, 2009.
[9] Malenkovic I, Eicher S, Bony J. Definition of Main System Boundaries and Performance Figures for Reporting on SHP Systems. ; 2012.
[10] Frank E, Haller M, Herkel S, Ruschenburg J. Systematic classification of combined solar thermal and heat pump systems. In Proceedings of the International Conference on Solar Heating, Cooling and Buildings 2010; 2010; Graz, Austria.